Supplemental Figure 1

A

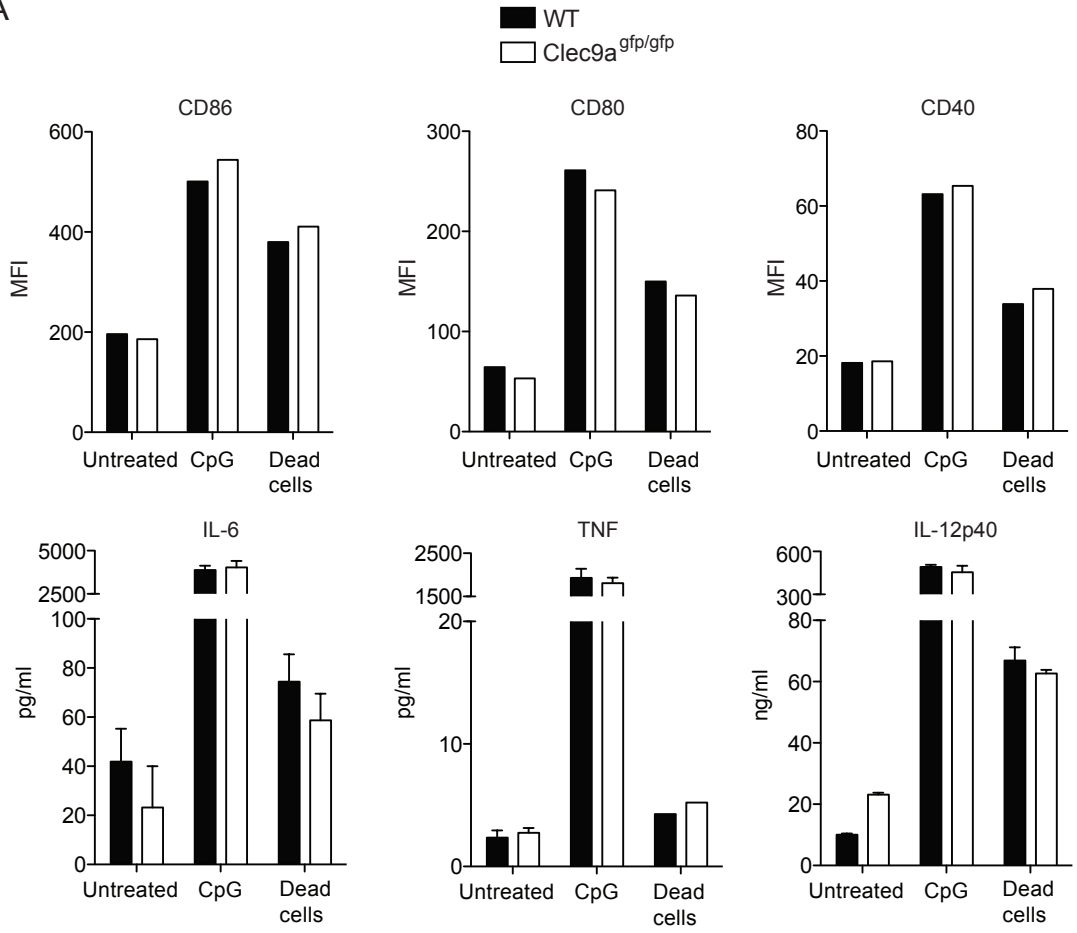

B

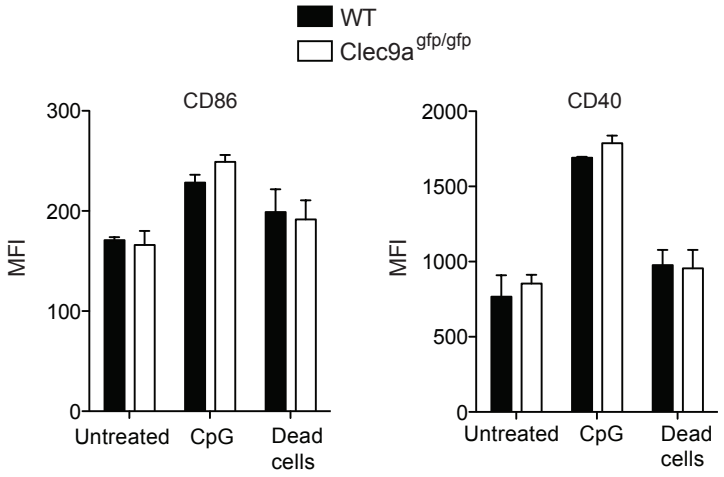

Supplemental Figure 1. Dead cells promote DC activation in a DNGR-1-independent manner. (A) Purified $CD8\alpha^+$-like Flt3L-BMDC from WT or DNGR-1-deficient ($Clec9a^{gfp/gfp}$) mice were cultured with UV-treated MEF (Dead cells) at a 1:1 ratio. MFI of CD86, CD80 and CD40 surface expression (upper panels) and concentration of IL-6, TNF-α and IL12/23 p40 in the supernatant (lower panels) were determined after overnight culture. As a positive control, DC were cultured in presence of CpG (500 ng/ml). (B) WT or DNGR-1-deficient ($Clec9a^{gfp/gfp}$) mice were left untreated or were injected with $5x10^5$ UV-treated MEF/mouse i.v. Spleens were analyzed the following day. MFI of CD86 and CD40 surface expression on $CD11c^+$ $MHC\text{-}II^+$ $CD8\alpha^+$ $CD11b^-$ live cells. As a positive control, mice were injected with 10 μg of CpG i.v.

Supplemental Figure 2

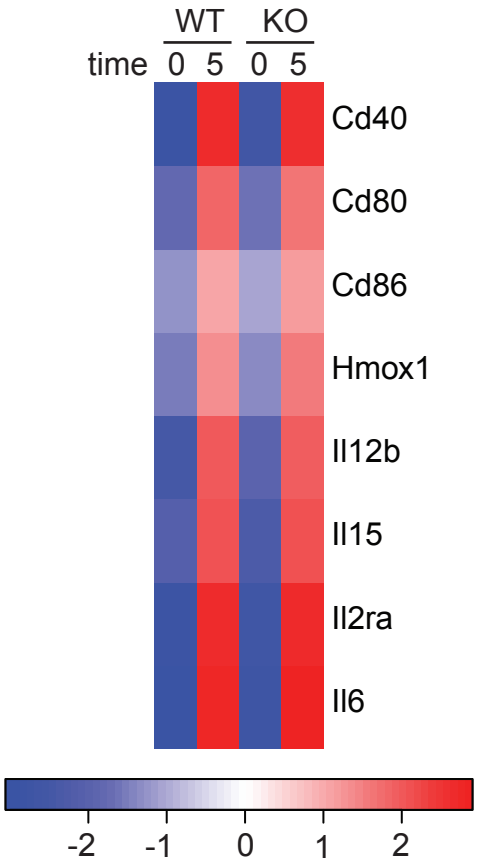

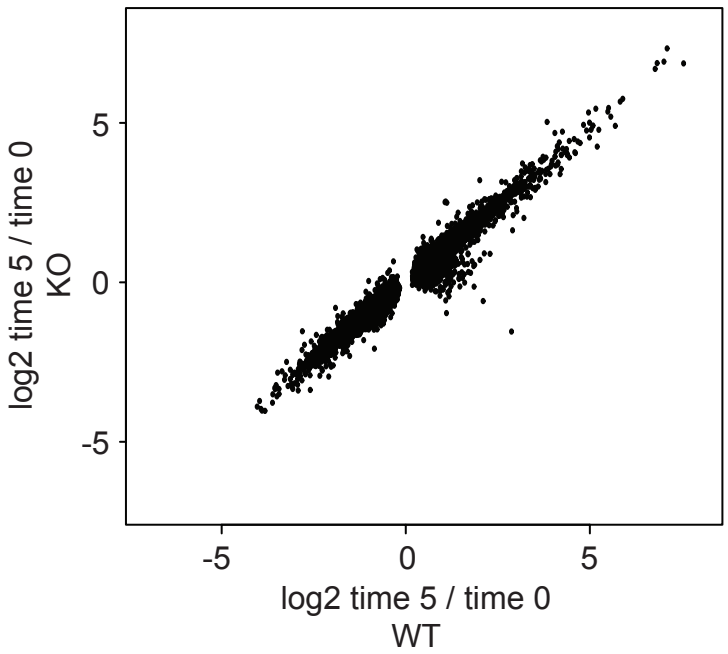

Supplemental Figure 2. Similar gene expression profile in WT and DNGR-1-deficient DC stimulated with dead cells. Flt3L-BMDC from WT or DNGR-1-deficient (KO) mice were left untreated (time 0) or were cultured for 5 hours with UV-treated MEF (time 5) at a 1:2 ratio. $CD24^{hi}$ $CD11b^{low}$ $B220^{-}$ $CD8\alpha^{+}$-like DC were purified by cell sorting and RNA was extracted. There were 3 replicates for each of the four experimental conditions. The samples were analyzed using Affymetrix MoEx-1_0-st-v1 exon arrays. The arrays were processed using the robust multi-array average algorithm and data were normalized to background. Quantification was carried out using Affymetrix Power Tools 1.10.0. A heatmap for selected genes (left panel) shows log2 replicate group mean signals for the four experimental conditions. Values are relative to the gene median signal across all conditions. Time point dependent gene changes for the WT group were identified by linear model using a 0.05 fdr threshold. The log2 ratios (time 5 versus 0) for these genes are shown for both the WT and KO groups in the scatter plot (right panel). A high concordance (Pearson correlation coefficient 0.9226) in the time point expression effect between the two groups is observed, indicating lack of any effect of DNGR-1 deficiency on dead cell-induced $CD8\alpha^{+}$-like DC gene expression. A few outlier dots do not reach statistical significance: the most prominent outlier dot corresponds to Olfr441 but analysis using a two-way ANOVA indicates that the gene is not differentially expressed.

Supplemental Figure 3

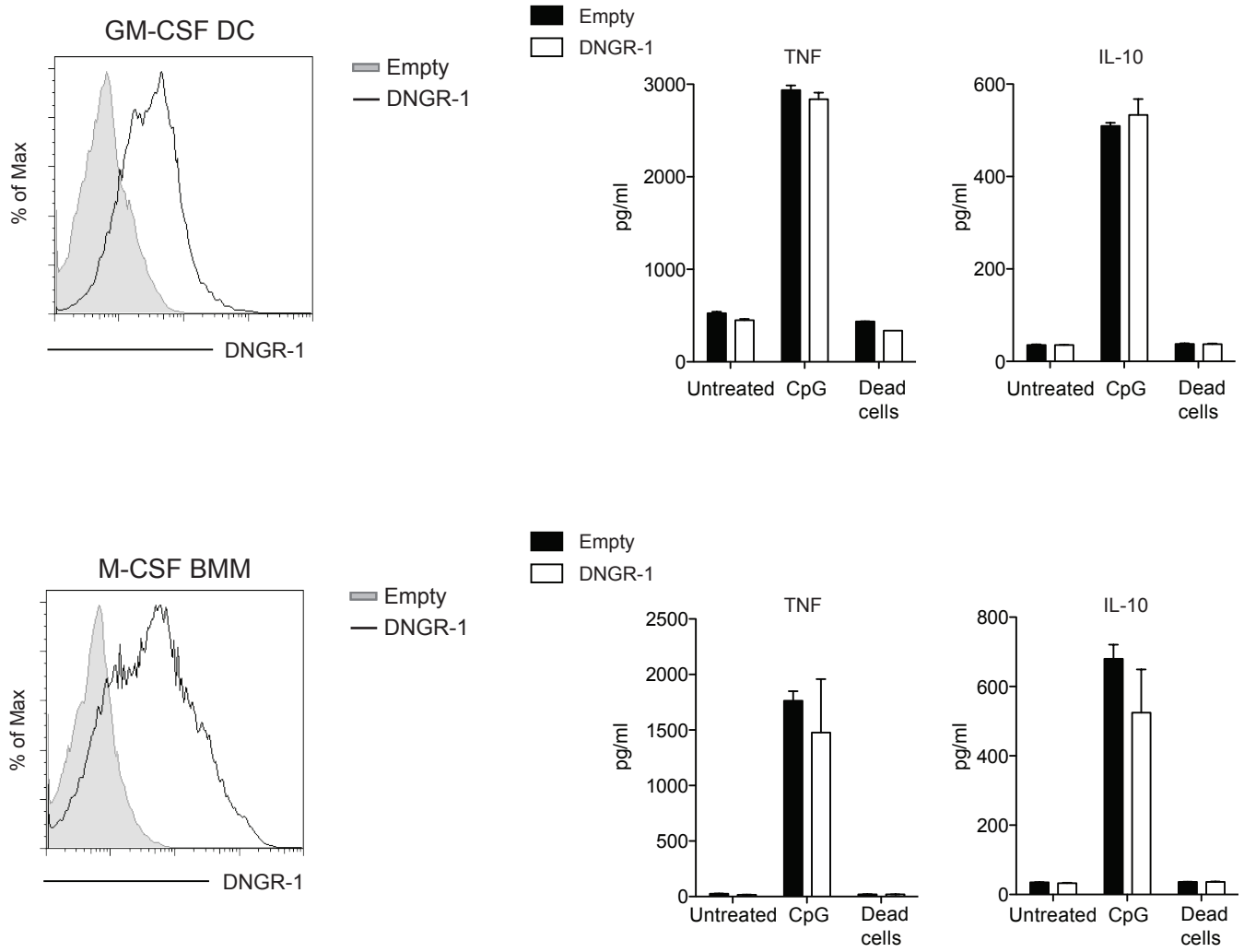

Supplemental Figure 3. Dead cells fail to activate GM-CSF DC or M-CSF BM-derived macrophages ectopically expressing DNGR-1. GMCSF BM derived DC (upper panels) or M-CSF BM derived macrophages (M-CSF BMM, lower panels) were retrovirally transduced with a control vector (Empty) or a vector encoding for DNGR-1. Expression of DNGR-1 by transduced cells as determined by staining with an anti-DNGR-1 antibody before stimulation (left panels). Concentration of TNF-α and IL-10 in the supernatant after overnight culture in presence of CpG (500 ng/ml) or UV-treated MEF (Dead cells) at a 1:1 ratio (right panels).

Supplemental Figure 4

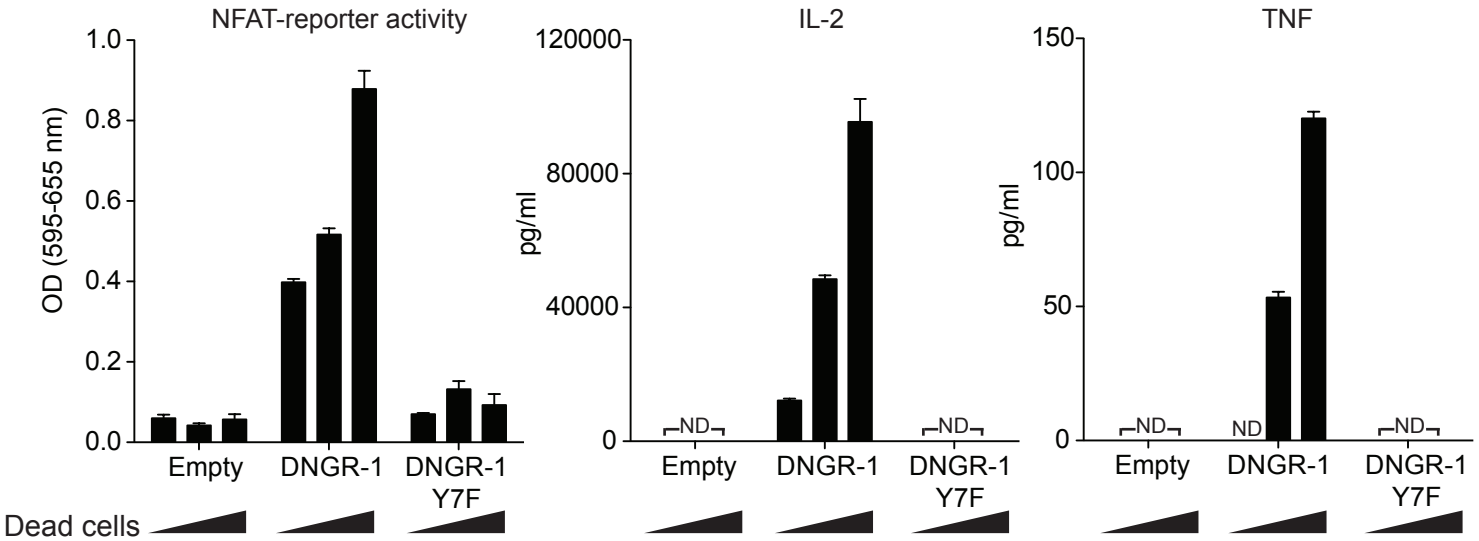

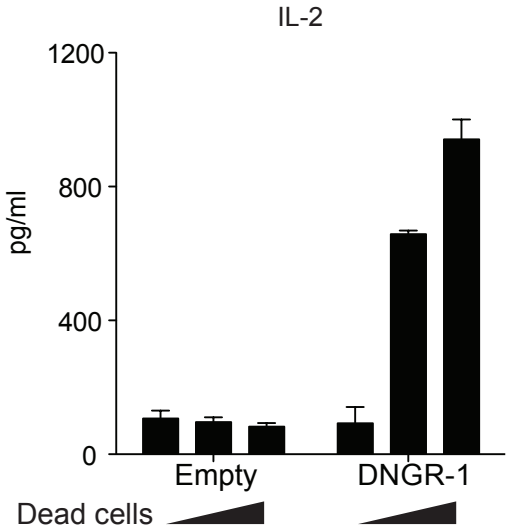

Supplemental Figure 4. DNGR-1 expression by B3Z or LK cells allows their activation by dead cells. Syk-expressing B3Z (upper panels) or LK (lower panel) cells stably transduced to express DNGR-1 or a mutant form of DNGR-1 (DNGR-1-Y7F) were cultured overnight in presence of increasing number of UV-treated MEF (Dead cells; ratio dead cells/responder cells: 0, 1:4 and 1:1). The concentration of IL-2 or TNF-α in the supernatant was determined by ELISA. N.D.: not detected.

Supplemental Figure 5

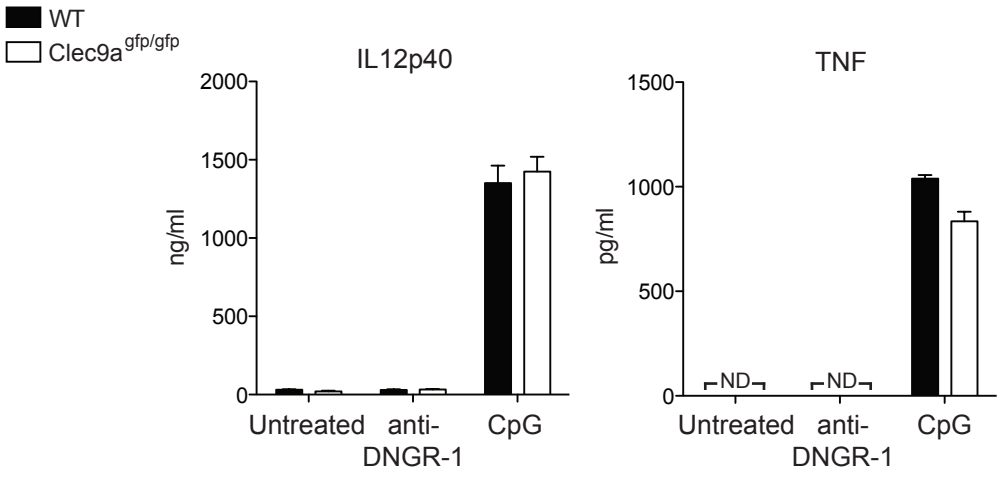

Supplemental Figure 5. Anti-DNGR-1 antibody does not activate DC. Purified CD8α^{+}-like Flt3L-BMDC from WT or DNGR-1-deficient (Clec9a$^{gfp/gfp}$) mice were cultured in presence of anti-DNGR-1 mAb (50 µg/ml, clone 7H11). IL12/23 p40 and TNF-α levels in the supernatant were determined after overnight culture. As a positive control, DC were cultured in presence of CpG (500 ng/ml).

Supplemental Figure 6

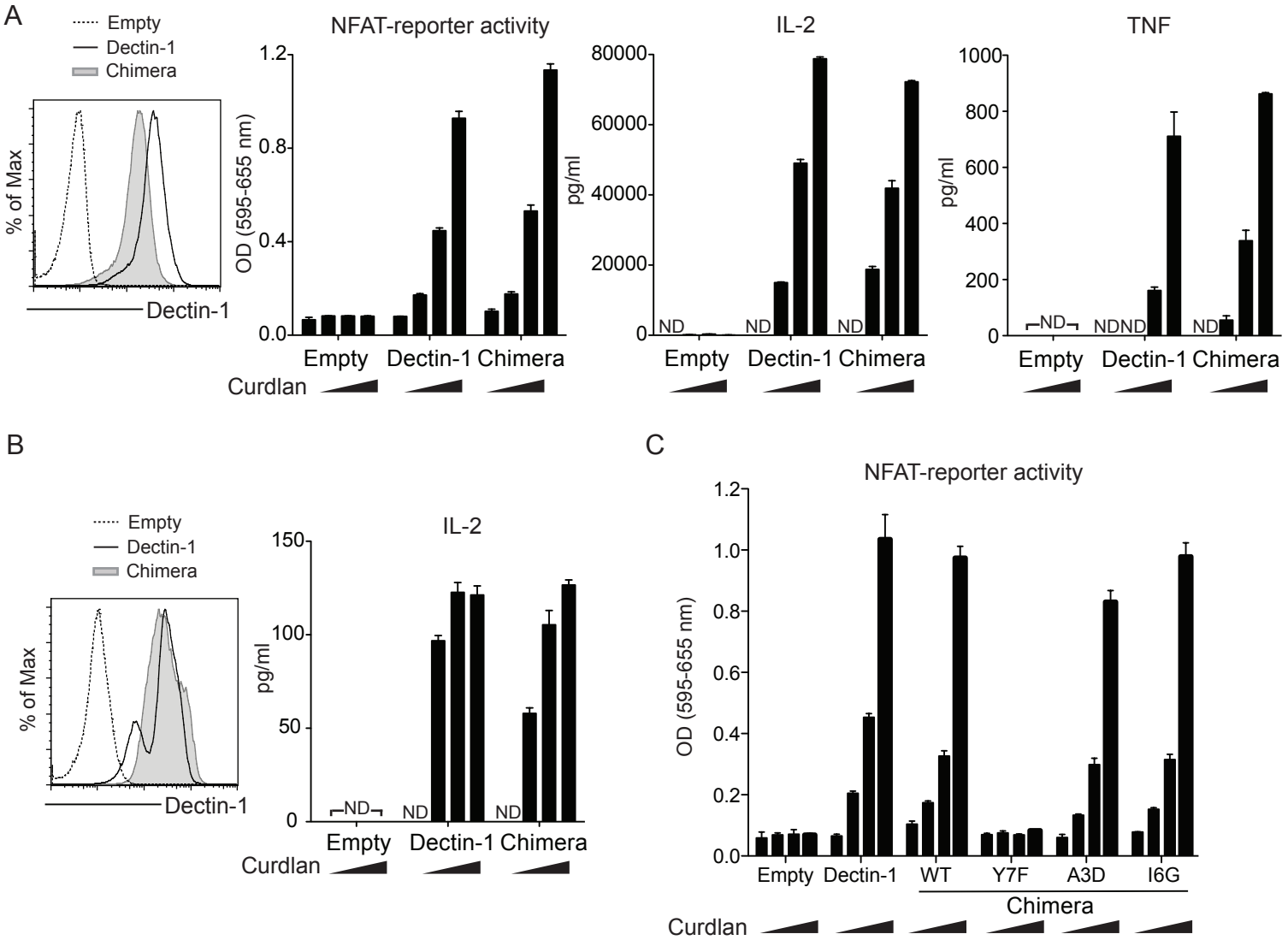

Supplemental Figure 6. A DNGR-1/Dectin-1 chimera activates B3Z and LK cells in response to curdlan. Syk-expressing-B3Z cells containing a reporter plasmid for NFAT coupled to LacZ were stably transduced to express Dectin-1 or a chimeric receptor (as in Figure 2A) and cultured overnight in presence of different amounts of curdlan (0, 20, 100 and 500 μg/ml). (A) Left panel: expression of Dectin-1 by B3Z cells before stimulation (Empty vector: dashed histogram, WT Dectin-1: solid histogram, Chimera: grey-filled histogram). Right panels: NFAT reporter activity and concentration of IL-2 and TNF-α in the supernatant. (B) LK cells were transduced with the same receptors and tested as in A. (C) NFAT reporter activity as in A with B3Z.Syk cells transduced with chimeric receptors bearing the Y7F, A3D or I6G mutation. Data are mean ± s.e.m and representative of at least 3 independent experiments. N.D.: not detected.

Supplemental Figure 7

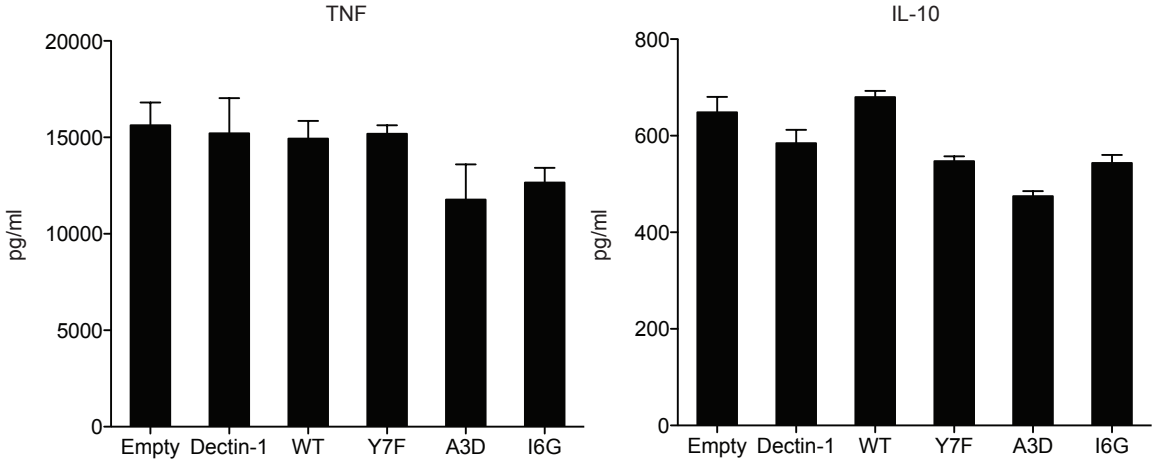

Supplemental Figure 7. Similar response of chimera-expressing DC to CpG stimulation. BM cells from Dectin-1-deficient mice were retrovirally transduced and purified as in Figure 2. Concentrations of TNF-α and IL-10 in the supernatant were determined after overnight culture in presence of CpG (500 ng/ml).

Supplemental Figure 8

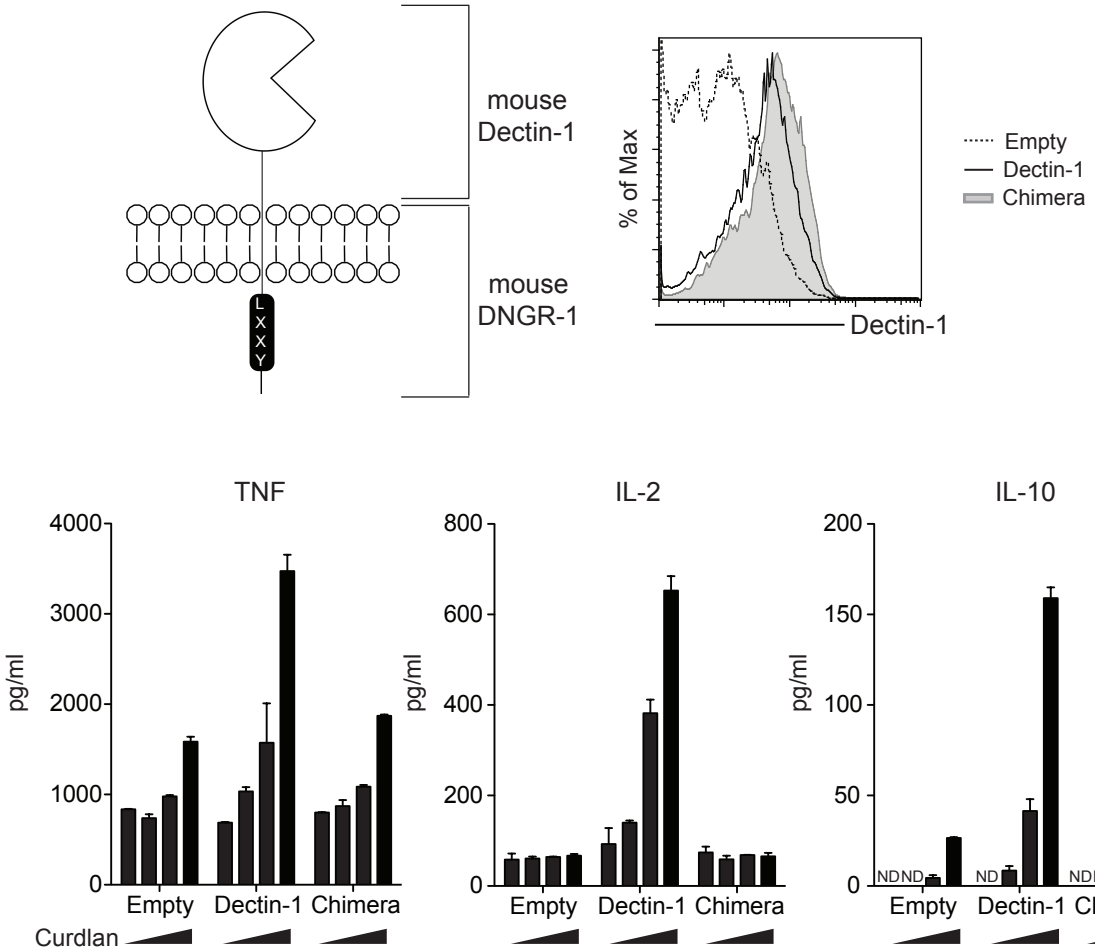

Supplemental Figure 8. A Dectin-1 chimeric receptor containing the cytoplasmic tail and the transmembrane domain of DNGR-1 does not activate DC in response to curdlan. BM cells from Dectin-1-deficient mice were retrovirally transduced with a vector encoding for GFP (Empty), Dectin-1 (Dectin-1) or a chimeric receptor (Chimera) bearing the cytoplasmic tail and the transmembrane domain of DNGR-1 fused to the stalk region and the CTLD of Dectin-1. All constructs were followed by an IRES-GFP sequence. After culture in presence of GM-CSF, GFP^+ cells were sorted to normalize for vector expression and further cultured overnight with increasing amounts of curdlan (0, 20, 100 and 500 µg/ml). Upper left panel, schematic representation of the chimeric DNGR-1/Dectin-1 receptor. Upper right panel, expression of Dectin-1 by DC after sorting and before overnight stimulation. Empty vector: dashed histogram, WT Dectin-1: solid histogram, Chimera: grey-filled histogram. Lower panels, TNF-α, IL-2 and IL-10 concentration in the supernatant. Data are mean ± s.e.m and representative of at least 5 independent experiments. N.D.: not detected.

Supplemental Figure 9

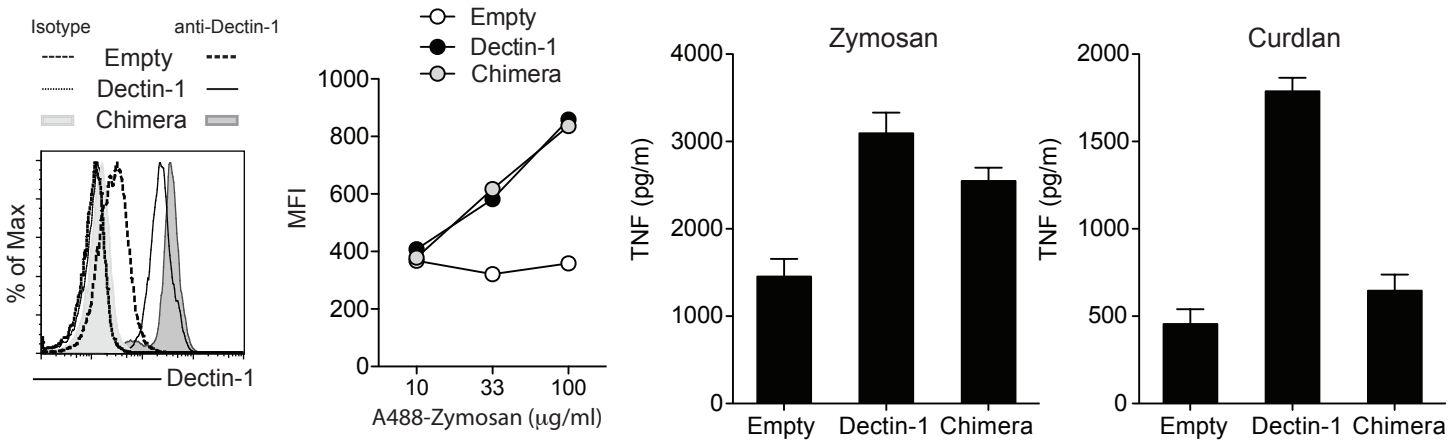

Supplemental Figure 9. A human DNGR-1/mouse Dectin-1 chimeric receptor does not mediate activation by a pure Dectin-1 agonist in RAW264.7 cells. RAW264.7 cells described before (36) were cultured for 1 hour at 4° C in presence of A488-labelled zymosan particles or overnight at 37° C in presence of curdlan or zymosan. Left panel, Dectin-1 expression by Raw264.7 cells before stimulation as detected with an anti-Dectin-1 mAb or with an isotype matched control. Middle panel, MFI of A488-zymosan-binding RAW264.7cells. Right panel, TNF-α concentration in the supernatant upon stimulation with 50 μg/ml of zymosan or 100 μg/ml of curdlan. Data are mean ± s.e.m and representative of 3 independent experiments.

Supplemental Figure 10

A

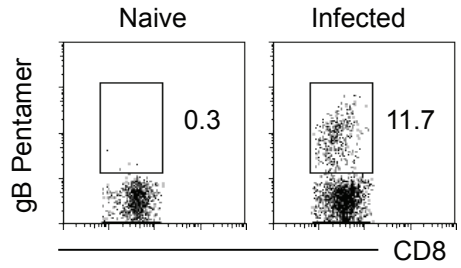

B

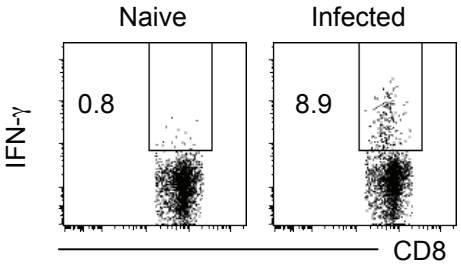

Supplemental Figure 10. Analysis of mediastinal lymph node T cell responses to HSV-1 infection. Mice infected with HSV-1 i.n. were sacrificed at 7 days and the mediastinal lymph nodes removed to analyze the magnitude of the endogenous gB-specific $CD8^+$ T cell response. (A) Cells were stained with mAbs specific for CD8, CD44 and H-$2K^b$-gB pentamer. Shown is a representative dot plot gated on $CD8^+$ $CD44^+$ cells from either a naïve or infected C57BL/6 mouse. (B) Mediastinal lymph nodes cells were re-stimulated with $gB_{498-505}$ peptide and stained with a mAb specific for CD8 and CD44 before being fixed, permeabilized and stained for IFN-γ. Shown is a representative dot plot gated on $CD8^+$ $CD44^+$ cells from either a naïve or infected C57BL/6 mouse.

Supplemental Figure 11

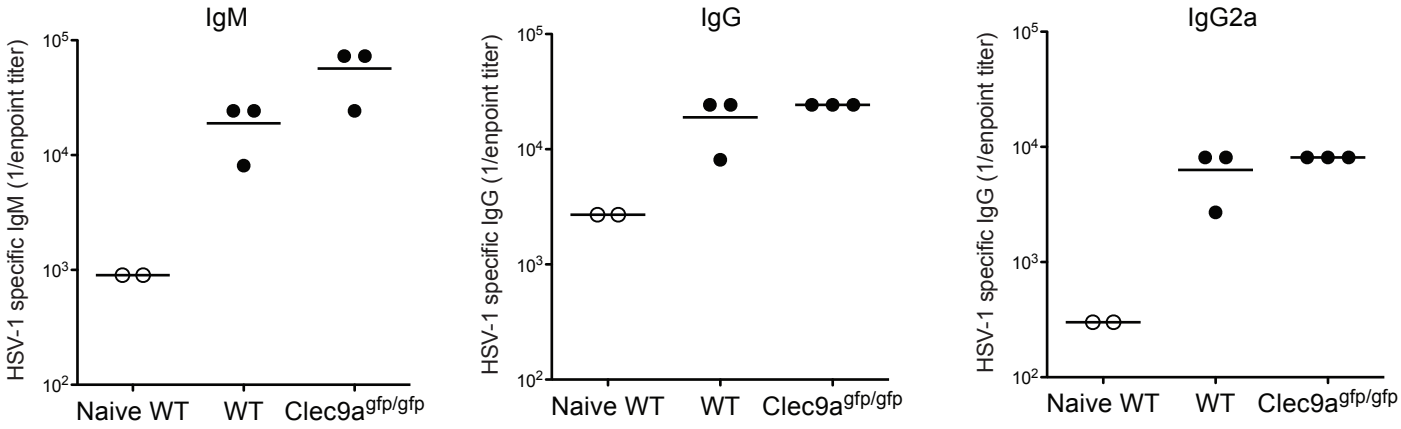

Supplemental Figure 11. DNGR-1 does not contribute to the Ab response to HSV-1 lung infection. WT or DNGR-1-deficient (Clec9a$^{gfp/gfp}$) mice were infected with HSV-1 i.n. The titer of HSV-1-specific IgM, IgG and IgG2a was determined by ELISA in sera 7 days post-infection. Each dot represents one mouse.

Supplemental Figure 12

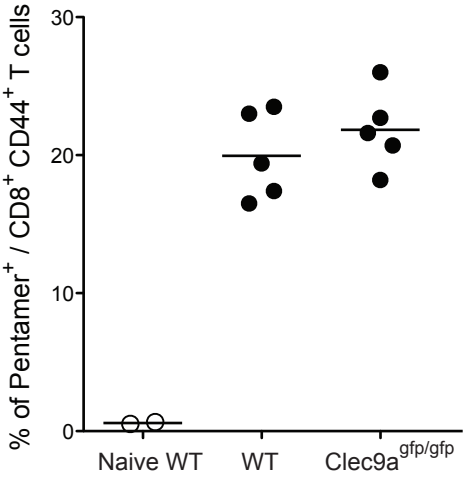

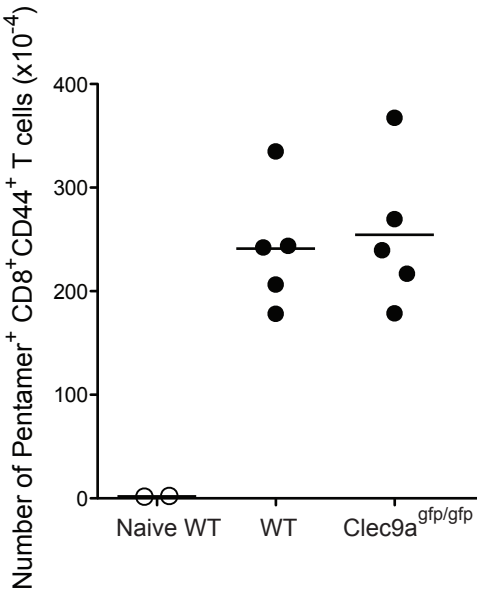

Supplemental Figure 12. DNGR-1 does not contribute to the CTL response to HSV-1 intravenous infection. WT or DNGR-1-deficient (Clec9a$^{gfp/gfp}$) mice were infected with HSV-1 i.v. Spleens were analyzed 7 days later. Percentage (left panel) and number (right panel) of H-2K^{b}-gB pentamer^{+} CD8^{+} CD44^{+} cells. Data are representative of 2 independent experiments with each dot representing one mouse.